CHAPTER V

HARTREE-FOCK PROJECTED SPECTRA

V.0 Introduction

The variational determinantal state obtained by the Hartree-Fock (HF) procedure is generally not an eigenstate of J^2 where J is the total angular momentum, and hence cannot be interpreted as one describing a particular state of the nucleus which is characterized by a definite J, since the Hamiltonian is invariant under rotations. It is therefore necessary to project out good angular momentum states from the HF intrinsic state so as to describe the actual states of nuclei. If the HF intrinsic state is highly deformed, it generates a "rotational band" and the good angular momentum states projected from it are related to each other as in the rotational model and can be interpreted as the collective rotational states of the nuclei.

We shall briefly discuss the method of angular momentum projection due to Peierls and Yoccoz[1] and evaluation of physical quantities like energies and electromagnetic properties for the levels in nuclear spectra employing projected wave functions. We shall briefly describe the orthonormalization procedure for states belonging to different bands generated by different HF intrinsic states of a nucleus. Since we shall be comparing our projected HF results with those of cranked HF formalism and

alpha-cluster model we shall outline briefly these two formalisms.

Since it is our aim to study the spectroscopic properties of some light mass nuclei using Skyrme interaction - both density independent and density dependent - we shall study energy spectra for the nuclei discussed in chapters III and IV by projecting out good angular momentum states from the HF intrinsic states. We shall study only the ground state spectra with the band-averaged scalar density dependent Skyrme interaction BASIV.

We recall that as mentioned in chapters III and IV, the HF calculations have been performed in the configuration space of first four oscillator major shells. Since all the nucleons are treated on equal footing, the core-polarization effects are automatically taken care of. We have assumed axial symmetry. Since it was found that the corrections arising due to centre-of-mass motion and Coulomb repulsion between protons do not contribute to the projected spectra significantly[36], these corrections are not incorporated in some cases in order to save the computational labour.

V.1 Projection of good angular momentum states.

Since we have assumed axial symmetry, the HF intrinsic state $|\phi_K\rangle$ is already an eigenstate of J_z with eigenvalue K, where J is the total angular momentum for the nucleus and Z-axis

is taken to be the symmetry axis of the nucleus.

$$J_z \mid \phi_K \rangle = K \mid \phi_K \rangle \qquad V(1)$$

If E is the energy corresponding to the variational state $\mid \phi_K \rangle$, we have,

$$\langle \phi_K \mid H \mid \phi_K \rangle = E$$
$$\langle \phi_K \mid \phi_K \rangle = 1 \qquad V(2)$$

Since the Hamiltonian is invariant under rotations, we have,

$$[R, H] = 0 \qquad V(3)$$

where R is the rotation operator. We therefore have,

$$E = \langle \phi_K \mid R^{-1} H R \mid \phi_K \rangle = \langle \phi_K \mid H \mid \phi_K \rangle$$

and

$$1 = \langle \phi_K \mid R^{-1} R \mid \phi_K \rangle = \langle \phi_K \mid \phi_K \rangle \qquad V(4)$$

which means that $\mid \phi_K \rangle$ and $R \mid \phi_K \rangle$ are degenerate. Following Peierls and Yoccoz[1], let us try to find the best superposition of the degenerate functions[2,3] $R(\Omega) \mid \phi_K \rangle$, where $\Omega \equiv (\alpha, \beta, \gamma)$ represents the Euler angles of rotation R,

$$\mid \psi_n \rangle = \int f_n(\Omega) R(\Omega) \mid \phi_K \rangle \, d\Omega \qquad V(5)$$

where,

$$R(\Omega) = e^{-i\gamma J_z} e^{-i\beta J_y} e^{-i\alpha J_z} \qquad V(6)$$

so that, $\langle \psi_n | H | \psi_n \rangle$ is a minimum with the constraint that $\langle \psi_n | \psi_n \rangle$ = constant. Then from the variational principle we have,

$$\delta \left[\langle \psi_n | H | \psi_n \rangle - E_n \langle \psi_n | \psi_n \rangle \right] = 0 \qquad V(7)$$

E_n is the Lagrange multipler giving energy of the state $|\psi_n\rangle$.

The answer to this problem is,

$$f_n(\Omega) = D^{J\,*}_{MK}(\Omega) \qquad V(8)$$

where $D^J_{MK}(\Omega)$ is the rotation matrix defined by

$$D^J_{MK}(\Omega) = \langle JM | R(\Omega) | JK \rangle \qquad V(9)$$

Substituting V(5) and V(8) in V(7), it can be shown that,

$$E_n = E_J = \frac{\int d\Omega \; D^{J\,*}_{MK}(\Omega) \langle \phi_K | R(\Omega) H | \phi_K \rangle}{\int d\Omega \; D^{J\,*}_{MK}(\Omega) \langle \phi_K | R(\Omega) | \phi_K \rangle} \qquad V(10)$$

The state n has good angular momentum J, Z component of the angular momentum M(in the space-fixed co-ordinate axes) and the band quantum number k. This state is denoted by $|\phi^J_{MK}\rangle$. Defining

$$P^J_{MK} = \frac{2J+1}{8\pi^2}\int D^{J*}_{MK}(\Omega)\ R(\Omega)\ d\Omega \qquad V(11)$$

as the projection operator projecting out the good angular momentum state $|\phi^J_{MK}\rangle$ from the intrinsic state $|\phi_K\rangle$, we can write

$$|\phi^J_{MK}\rangle = \frac{2J+1}{8\pi^2}\cdot\frac{1}{N^{J1/2}_{KK}}\int d\Omega\ D^{J*}_{MK}(\Omega)\ R(\Omega)\ |\phi_K\rangle \qquad V(12)$$

where N^J_{KK} is the normalization constant given by

$$N^J_{KK} = \frac{2J+1}{8\pi^2}\int d\Omega\ D^{J*}_{KK}(\Omega)\ \langle\phi_K|R(\Omega)|\phi_K\rangle \qquad V(13)$$

Since we assume axial symmetry in our calculations, it can be shown that V(10) reduces to,

$$E_J = \langle \phi^J_{MK}\ |H|\ \phi^J_{MK}\rangle$$

$$= \frac{\frac{2J+1}{8\pi^2}\int_0^{\pi} d\beta \sin\beta \; d^J_{KK}(\beta) \langle \phi_K | e^{-i\beta J_y} H | \phi_K \rangle}{\frac{2J+1}{8\pi^2}\int_0^{\pi} d\beta \sin\beta \; d^J_{KK}(\beta) \langle \phi_K | e^{-i\beta J_y} | \phi_K \rangle}$$

$$= H^J_{KK} / N^J_{KK} \qquad \text{V(14)}$$

To calculate E^J, one needs to evaluate $\langle \phi_K | e^{-i\beta J_y} H | \phi_K \rangle$ and $\langle \phi_K | e^{-i\beta J_y} | \phi_K \rangle$ in V(14). Warke and Gunye[4] have explicitly derived the expressions to calculate these quantities for axially symmetric nuclei. We use their expressions in our calculations.

For a well deformed nucleus i.e. when $| \phi_K \rangle$ is strongly deformed, the energies E_J are shown to be related as in rotational model[5]. The functions $| \phi^J_{MK} \rangle$ then correspond to **rotational** states of the intrinsic state $| \phi_K \rangle$. If $| \phi_K \rangle$ does not contain rotational states, P^J_{MK} would still project out states with good J, but, they will not be related as rotational states.

V.1.1 Orthonormalization of the projected states belonging to different bands.

When there are two or more than two HF intrinsic states

$|\Phi_K\rangle$ lying close in energy, each $|\Phi_K\rangle$ gives rise to a band of good J states characterized by the band quantum number K. Good J states belonging to different K bands, however, may not be orthogonal to each other and therefore it is necessary to orthonormalize them. This is invariably the case with odd-odd nuclei. One way to orthonormalize these states is the well-known Schmidt's orthogonalization procedure, but, this is quite cumbersome when the number of states is quite large. We therefore use an alternative method which requires the solution of the matrix diagonalization equation

$$\left[H^J - \epsilon^n_J N^J \right] {}^nC^J = 0 \qquad V(15)$$

where H^J is the energy matrix defined by the matrix elements $H^J_{k_1 k_2}$ etc. and N^J is the overlap matrix defined by $N^J_{k_1 k_2}$ etc. as defined in eqn. V(14). ${}^nC^J$ is the column vector which gives the "mixing" from various non-orthonormal states in the state with good angular momentum J. If we consider only two bands defined by the quantum numbers K_1 and K_2, we can write

$$|J\rangle = {}^nC^J_{K_1} |JK_1\rangle + {}^nC^J_{K_2} |JK_2\rangle \qquad V(16)$$

corresponding to energy ϵ^n_J in V(15).

One can then calculate various quantities of interest like electric quadrupole moment, magnetic dipole moment, transitions etc. in the band-mixed state $| J \rangle$.

V.1.2 Calculation of electromagnetic properties with projected wave functions.

In this section we shall quote a general expression[4,5] for the matrix element $\langle \phi^{J_1}_{M_1 K_1} | T^k_q | \phi^{J_2}_{M_2 K_2} \rangle$ for a tensor operator T^k_q and state how it can be used to calculate the electromagnetic properties. In Ref.(5), it is shown that

$$\langle \phi^{J_1}_{M_1 K_1} | T^k_q | \phi^{J_2}_{M_2 K_2} \rangle$$

$$= \left[(2J_2+1) / 8\pi^2 \left(N^{J_1}_{K_1 K_1}\right)^{1/2} \left(N^{J_2}_{K_2 K_2}\right)^{1/2} \right]$$

$$\times C \begin{bmatrix} J_2 & k & J_1 \\ M_2 & q & M_1 \end{bmatrix}$$

$$\times \sum_{\mu\nu} C \begin{bmatrix} J_2 & k & J_1 \\ K_2 & \nu & \mu \end{bmatrix} \int d\Omega \, D^{J_1 *}_{K_1 \mu}(\Omega) \langle \phi_{K_1} | R(\Omega) T^k_\nu | \phi_{K_2} \rangle$$

V(17)

where the quantities in square brackets are the usual Clebsch-Gordon coefficients. The expression V(17) can be used depending on the quantity to be evaluated. For example, the electric

quadrupole moment and the magnetic dipole moment in the projected state $|\phi^J_{MK}\rangle$ can be calculated by evaluating the matrix elements

$$\langle \phi^J_{MK} | Q^2_0 | \phi^J_{MK} \rangle \text{ and } \langle \phi^J_{MK} | \mu^1_0 | \phi^J_{MK} \rangle$$

respectively. Here Q^2_0 is the electric quadrupole operator defined by

$$Q^2_0 = \sum_{i_1, i_2}^{\text{Protons}} e \sqrt{\frac{16\pi}{5}} \langle i_1 | r^2 Y_{20}(\theta, \phi) | i_2 \rangle a^+_{i_1} a_{i_2} \qquad \text{V(18)}$$

and μ^1_0 is the magnetic dipole operator defined by

$$\mu^1_0 = \sum_{i_1, i_2} \langle i_1 | g^{(l)} l_z + g^{(s)} s_z | i_2 \rangle a^+_{i_1} a_{i_2} \qquad \text{V(19)}$$

where l_Z and S_Z are the Z-components of the orbital and spin angular momentum respectively. $g^{(l)}$ and $g^{(s)}$ are the orbital and spin g-factors for a nucleon. $g^{(l)}$=1 for proton and 0 for neutron , $g^{(s)}$=5.5855 for proton and -3.8270 for **neutron.** E2 and

M1 transition amplitudes can be calculated in a similar fashion using the expression V(17).

V.1.3 An outline of self-consistent Cranking model.

In the section V.4.1 we shall compare our results of projected HF calculations for ^{20}Ne with those of self-consistent cranking model (CHF) and hence for the sake of completeness, we outline below the method of CHF to study the rotational states of nuclei.

In CHF, one solves the constrained Schrödinger equation,

$$H_\omega |\phi_\omega\rangle = E_\omega |\phi_\omega\rangle \qquad V(20)$$

with

$$H_\omega = H - \omega J_x \qquad V(21)$$

where H_ω is treated in the HF approximation. H is the nuclear Hamiltonian and J_x is the x-component of the total angular momentum $\vec{J}$. ω is a Lagrange multiplier. To each wave function $|\phi_\omega\rangle$ one assigns an angular momentum J such that

$$\sqrt{J(J+1)}\hbar = \langle \phi_\omega | J_x | \phi_\omega \rangle \qquad V(22)$$

The calculations need to be carried out separately for each J in question.

It has been shown[6,7] that the CHF procedure can be looked upon as being equivalent to a prescription which would lead to a minimization of energy for each J individually. This is, however, true only under certain conditions which essentially imply only small departure of $|\phi\omega\rangle$ from axiality and that the nucleus to be strongly deformed. Explicit calculations have shown that CHF procedure when applied to 2s-1d and 2p-1f shell nuclei can be viewed merely as a prescription to obtain approxi mate behaviour of a rotational spectrum[8]. However, the CHF formalism has been applied to obtain anomalous behaviour of high spin states in heavy nuclei[9].

V.1.4 An outline of the alpha-cluster model of the nucleus.

In sections V.3 and V.3.1 we shall study the ground state spectra of ^{12}C and compare our projected HF results with those of alpha-cluster model. We shall therefore give an outline of the alpha-cluster model described by Brink[10] in this section. This model includes in a simple way four nucleon correlations. In a nucleus with A=4n, one takes a set of n single-particle wave functions

$$\phi_i(\vec{r}) = [b^3 \pi^{3/2}]^{-1/2} \cdot \exp\left[-(\vec{r} - \vec{R}_i)^2 / 2b^2\right] \cdot \eta$$

$$i = 1, 2, \ldots, n \qquad \text{V(23}$$

η is one of the four spin-isospin wave functions. Antisymmetrized product of four such wave functions describe alpha-particle like configuration at the point $\vec{R}_i$. The 4n nucleon state is described by forming the 4n particle normalized Slater determinant $\Phi(\vec{R}_1, \vec{R}_2, \ldots \vec{R}_n)$ from the η alpha-cluster wave functions. There is a tendency for two protons and two neutrons to cluster about each of the points $\vec{R}_i$, but, this clustering is inhibited if the points $\vec{R}_1, \vec{R}_2, \ldots \vec{R}_n$ are quite close to each other because of the exclusion principle. The size of the clusters is determined by the parameter b. Since all clusters have zero spin, the contribution due to the spin-orbit force is identically zero. In the alpha-cluster calculations, all the nucleons are treated on equal footing just as in the multishell HF calculations. In general, alpha-cluster wave functions $\Phi(\vec{R}_1 \ldots \vec{R}_n)$ do not have good parity or good angular momentum and thus it is necessary to remedy this by projecting out states of good parity and good angular momentum.

V.2 Spectra of some A=8 nuclei with:

(i) density independent Skyrme and

(ii) Sussex interaction.

Numerous shell model calculations[11-15] for the 1p shell nuclei assuming the configuration to be $(1s)^4(1p)^{A-4}$ have been reported in literature. Dirim et al[16] have reported shell model

calculations with the modified Sussex interaction[17] incorporating a hard-core potential for 1p shell nuclei. These calculations, however, are very cumbersome and also up to four valence nucleons, the hard-core effects are small[16]. All the calculations, however, have met with only limited success due to the neglect of expected large core-polarization effects in this region. In order to incorporate core-polarization effects, calculations in a large model space are essential. Such projected multishell HF calculations for a few nuclei in this region were reported by Gunye et al[18] with the original Sussex interaction in the configuration space of first four major shells. We have performed calculations here for some A=8 nuclei with the original Sussex interaction since the hard-core effects are small for these nuclei as shown in Ref.16.

In this section we shall study the projected spectra for the nuclei ^{8}Li, ^{8}Be and ^{8}B obtained from their HF intrinsic states already described in chapter III with SV and Sussex interactions[19,20]. As mentioned before, the configuration space consists of first four major shells. Also since all the particles are treated on the same footing, core-polarization effects are automatically taken care of. The oscillator parameter value b = 1.7 fm was used. This is the optimized b value for the interaction SV for A=8 nuclei. Sussex interaction does not show a severe b dependence[18] as does the Skyrme interaction

due to the truncational effects of the configuration space and hence the value of b=1.5 fm was used. The corrections due to centre-of-mass motion and the Coulomb repulsion between protons have been explicitly incorporated in these calculations.

Nuclei ^{8}Li and ^{8}B

These nuclei being the mirror nuclei, their spectra are expected to be identical except for the differences arising out of the Coulomb repulsion. Experimentally more data is available for ^{8}Li than for ^{8}B. For both the nuclei the ground state has $J=2^{+}$ and T=1.

For both the nuclei, two HF solutions with band quantum number K=1 and K=2 are obtained which lie close in energy as shown in tables III.3A and III.3B in chapter III with SV as well as with Sussex. Hence it is necessary to orthogonalize the projected good angular momentum states from both the bands and calculate various quantities of interest for comparison with experiment in the band mixed state. We show in Figs.V(1) and V(2) the spectra obtained for ^{8}Li and ^{8}B respectively with the interactions SV and Sussex and compare them with the experiment.

It is seen from the Fig.V(1) and V(2) that the energy spectra obtained with Sussex interaction are in a better agreement with the experimental ones as compared to the spectra obtained with the interaction SV, although SV provides a better

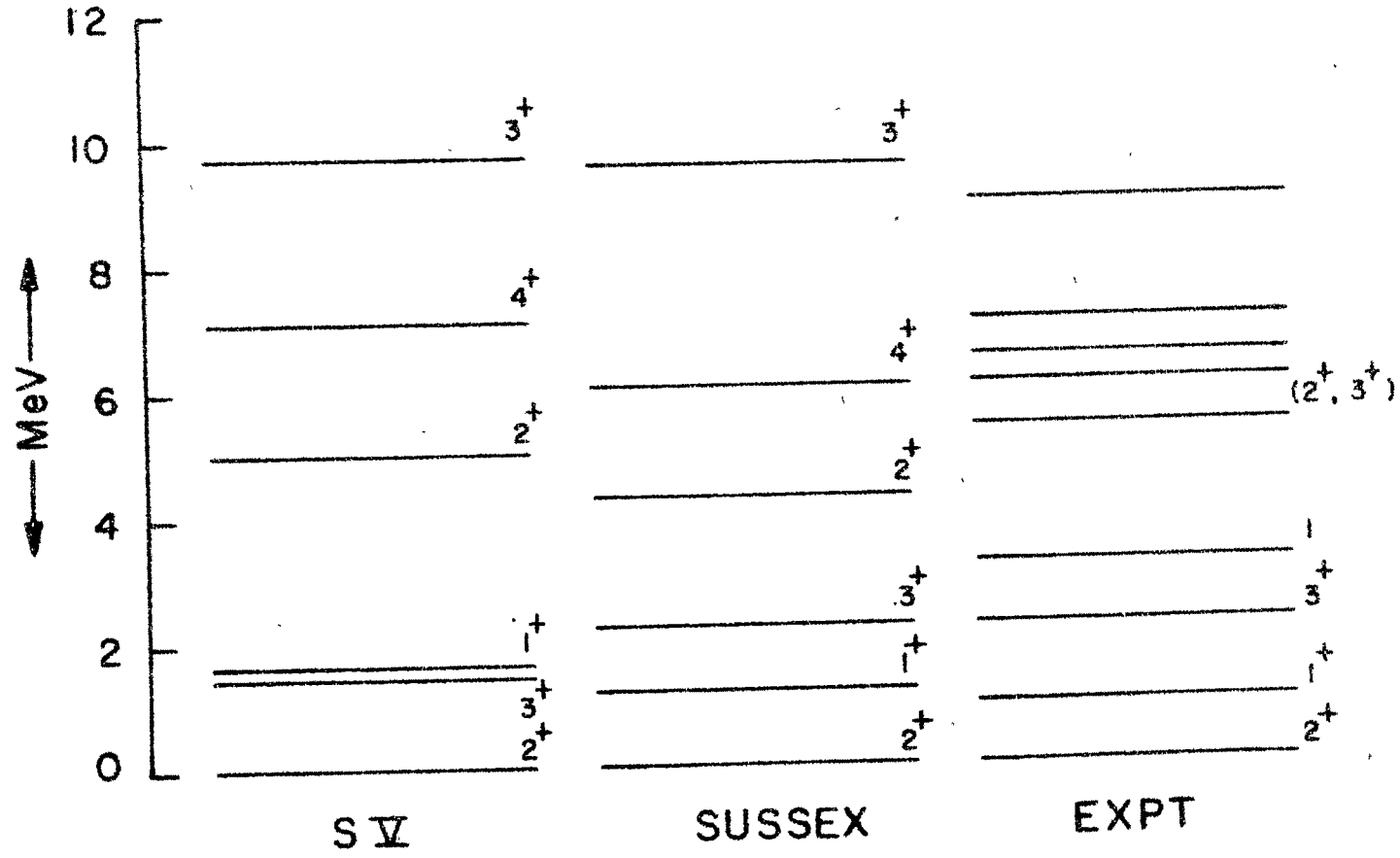

Fig.V(1): ^{8}Li energy spectra

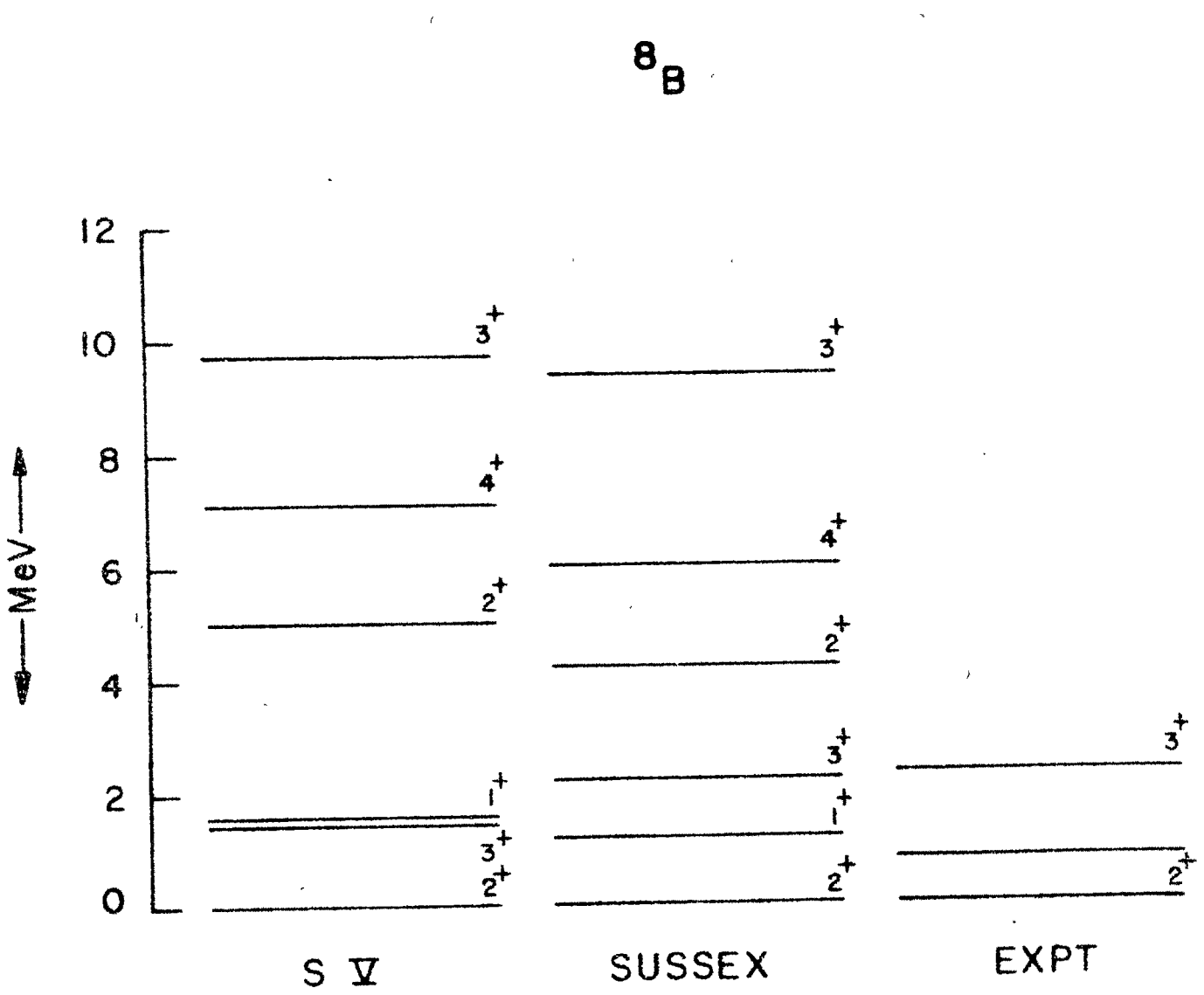

Fig.V(2): ^{8}B energy spectra

binding for these nuclei as seen in chapter III. The levels 1^+ and 3^+ which are well reproduced by Sussex have changed their ordering when calculated with SV. However, it is seen from the experimental spectrum for ^{8}Li that to obtain states other than the ground state band we have to mix some more particle-hole excitations. The results for the Skyrme interaction may be improved by incorporating density dependence in the interaction.

We have calculated the magnetic dipole moment and the electric quadrupole moment in the ground state of these nuclei i.e. $J^{\pi} = 2^+$, $T = 1$ in the band-mixed state. We have displayed the results in table V.1 . The calculated values of the magnetic dipole moment compare well with experiment for Sussex for both ^{8}Li and ^{8}B. SV gives a reasonably good value for the magnetic dipole moment of ^{8}Li, but, highly underestimates the same for ^{8}B. The calculated value for electric quadrupole moment for ^{8}Li also compares well with experiment for Sussex, but, is highly underestimated for SV. Unfortunately, the experimental value for the electric quadrupole moment for ^{8}B is not available at the moment. In view of the total unavailability of the experimental data for electromagnetic transitions and the need to include some more particle-hole excitations in theoretical calculations for a better description of these properties, we shall not give the calculated values of the reduced transition rates, B(E2) and B(M1) for these nuclei.

TABLE V.1

Ground state properties of ^{8}Li and ^{8}B

Nucleus	J^{π}	Int.	μ_{nm} (cal.)	μ_{nm} (expt.)	Q_{mb} (cal.)	Q_{mb} (expt.)[39]
^{8}Li	2^{+}	Sussex	1.5640	1.65335±0.00035[37]	23.97	32±6
		SV	1.4705		0.63	
^{8}B	2^{+}	Sussex	1.09	1.0355±0.003[38]	31.0	-
		SV	0.6243		8.01	

The nucleus ^{8}Be

For this nucleus we obtain only the ground state band with K=0 with both SV and Sussex interactions. We give the energy of the 0^{+} level in table V.2. We present the projected spectra with these interactions in Fig.V(3) and compare with the experimental one. It is seen that in this case also the Sussex interaction gives a better description of the ground state band. The ground state band obtained with SV is somewhat compressed. In the experimental spectrum, one excited K=0 band can also be seen which can be obtained by mixing some higher particle-hole excitations in the calculation.

We conclude this section with the note that the Sussex interaction offers a better description of the nuclei ^{8}Li, ^{8}Be and ^{8}B than does SV. To obtain better agreement with experiment, it may be necessary to perform calculations incorporating density dependence in Skyrme interaction, which as we shall show in sections V.4 and V.4.1, is found to be important for nuclei like ^{8}Be, ^{12}C and ^{20}Ne.

V.3 Role of two-body spin-orbit interaction in the structure of ^{12}C.

We studied the projected spectra for some A=8 nuclei in the preceeding section with the density independent Skyrme interaction SV. It would be however quite interesting to see if

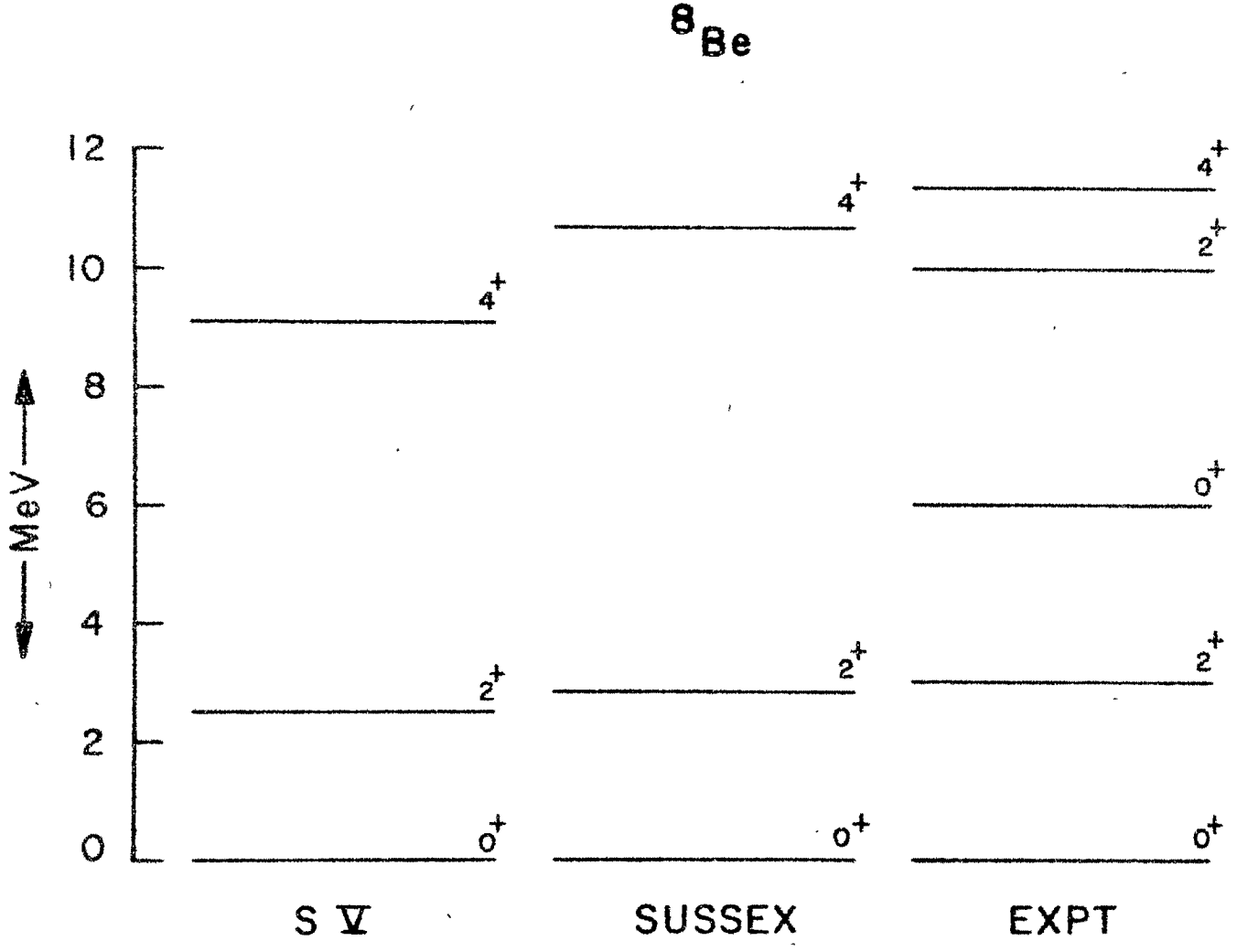

Fig.V(3): ^{8}Be energy spectra

TABLE V.2

HF Results for ^{12}C and ^{8}Be

Interaction	Nucleus	E_{HF} MeV	Q_{o_2} fm^2	RMS fm	RE. EN MeV	E_{0^+} MeV
SV(Oblate)	^{12}C	-76.22	-32.50	2.56	-	-81.18
SV(W=0)		-70.95	-37.88	2.63	-	-74.41
SV(Prolate)		-72.45	14.35	2.51	-	-74.40
Sussex		-33.11	-27.32	2.27	-	-37.58
BASIV		-81.70	-36.31	2.56	-15.96	-87.50
Expt.		-92.2	-	2.40 ± 0.03[34] 2.447[22]		
SV	^{8}Be	-36.34	39.71	2.52	-	-40.46
BASIV		-42.94	47.19	2.54	-6.44	-49.18
Expt.		-56.50				

one can obtain information about the various parameters of the Skyrme interaction by calculating spectroscopic properties and see if certain spectroscopic properties are sensitive to some of the parameters in the force. In this section we show that in the case of ^{12}C spectrum, such sensitivity exists with respect to the two-body spin-orbit part of the interaction[25]. one can not overemphasize the importance of this part of the two-body interaction as the vital single-particle spin-orbit field leading to j-j coupling shell model arises from it. Indeed from the calculations of Kurath[11] it is clear that the spacing between the energy levels of ^{12}C is sensitive to the strength of the spin-orbit field. He observed that the spacing between energy levels increased by increasing the one-body spin-orbit strength. He could obtain reasonable agreement with the experimental spectrum only when the spin-orbit strength was taken too large.

Previous calculations[21,22] using Skyrme interactions with a strong density dependence give a spherical HF ground state with zero intrinsic quadrupole moment for ^{12}C. The projected spectra from alpha-cluster calculations can not take account of the spin-orbit interaction and are rather compressed[23,24]. We have chosen the Skyrme variant SV (which has $t_3=0$) for the present calculations. We obtained the oblate and prolate HF solutions for ^{12}C. The intrinsic quadrupole moments, r.m.s. radii, energies and energy of the 0^+ state are given in Table V.2. The interaction

SV has a rather strong spin-orbit term (W=150 MeV fm^5). We also carried out HF calculation by putting its strength equal to zero. The intrinsic properties of two solutions are tabulated in Table V.2. One can see that the spin-orbit interaction contributes about 5 MeV to the binding energy i.e. about 7% of the total binding energy and leads to somewhat less deformed solution. Eventhough there is some underbinding and slight overestimation of the r.m.s. radius, these results are much better than those with Sussex also shown for comparison. We did not include corrections due to centre-of-mass motion and Coulomb repulsion between protons since their effect on projected spectra is quite negligible[36].

The projected good angular momentum states from the HF solution for the ground state band are shown in Fig.V(4). The agreement with experimental results with SV is quite good (A), while removal of spin-orbit interaction leads to the rather compressed spectrum (B) resembling one obtained in the alpha-cluster model[33]. We also made an explicit calculation by putting W=0 in the projection calculation to estimate the contribution of the spin-orbit part of the interaction to the ^{12}C spectrum with HF wave function obtained by including spin-orbit interaction. It was found that out of the (0^+-2^+) separation (4.59 MeV) the contribution of the two-body spin-orbit force alone is 3.8 MeV. The electric quadrupole moment, the reduced transition rate

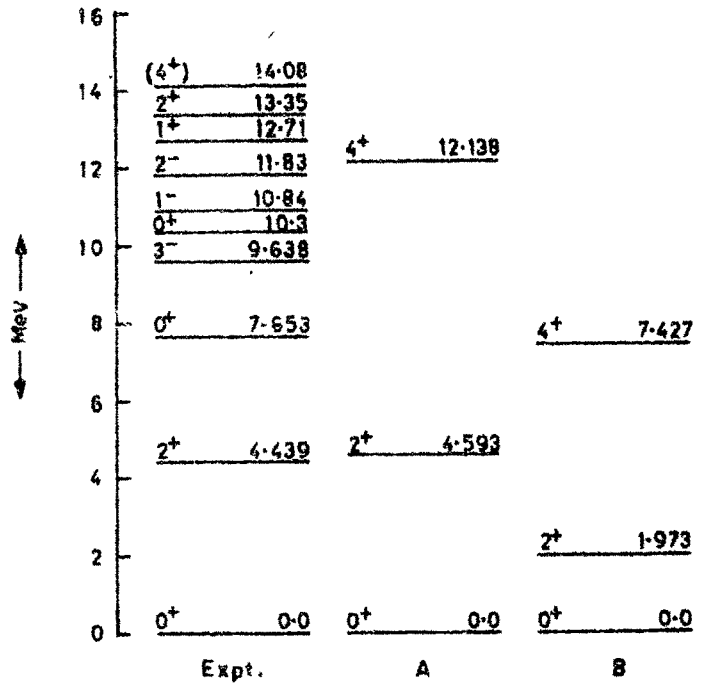

Fig.V(4): ^{12}C energy spectra with
(A) interaction SV and
(B) omitting spin-orbit contribution from SV.

$B(E2, 0^+ \rightarrow 2^+)$ and the magnetic dipole moments are shown in Table V.3. The agreement of the reduced transition rate B(E2) calculated with SV with the experiment is quite good while W=0 results are overestimated. It may be of interest to note that projected states from prolate solution are pushed up considerably after orthogonalizing with the oblate band.

We hence see that the two-body spin-orbit interaction plays a very important role in explaining the ground state energy spectrum of ^{12}C.

V.3.1 Comparison with alpha-cluster model

In this section we shall compare our results of deformed HF calculation with those of alpha-cluster model for ^{12}C described in section V.1.4. This can be most conveniently done by comparing HF wave function with that of alpha-cluster model by calculating the overlap between the two. We calculated the overlaps of HF wave functions with the positive parity wave functions projected from an alpha-cluster configuration of equilateral triangle type in Brink's model[10]. The overlaps were obtained as a function of the cluster separation R, the distance between vertex and the centroid of the triangle. As seen in Fig.V(5), the HF solution with spin-orbit interaction has smaller overlap at all cluster separations with a maximum at R=0, while the maximum for the HF solution with W=0 lies at finite separation ($R \sim 1.2$ fm). It

TABLE V.3

ELECTROMAGNETIC PROPERTIES OF ^{12}C

Interaction	Q $(J = 2^+)$ e fm^2	μ $(J = 2^+)$ nm	$B(E2, 0^+ \longrightarrow 2^+)$ Cal. $e^2 fm^4$	Expt 35)
BASIV	5.9048	0.7718	46.88	42.3±3
SV	5.4942	0.7297	39.8	-
SV(W=0)	6.4915	0.6372	51.1	

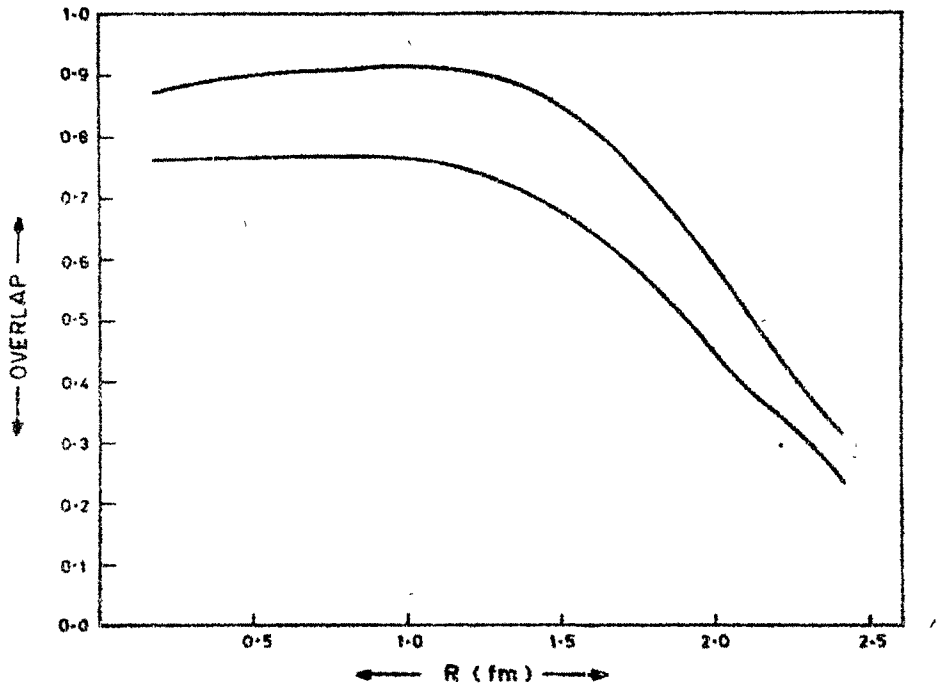

Fig.V(5): The overlap of the alpha-cluster wave functions with the HF wave functions.

should be noted that the HF energies with and without W contributions are ~ 9 and 4 MeV lower than the alpha-cluster model energies. It seems therefore that HF description improves upon the cluster model; more so in the presence of the spin-orbit interaction. It should be noted that in spite of the repulsive nature of SV in p-state, the clustering is very little especially in the presence of the spin-orbit interaction. The alpha clustering in a linear chain may still be invoked to give description of some excited states as it was found that the states projected from the prolate HF solution have large overlaps with the states projected from the oblate HF solution.

We thus see that the energy separations as well as the structure of low-lying levels of ^{12}C are profoundly affected by the two-body spin-orbit part of the interaction[25]. In fact, this effect is expected for all nuclei neighbouring ^{12}C since the nucleons can be scattered to $1p_{1/2}$ orbit from $1p_{3/2}$ orbit which is almost full and the former empty.

We may note in this section that due to inadequate spin-orbit force in Sussex interaction in the ^{12}C region, the spectra obtained with this interaction are quite compressed. If we make $(1p_{3/2})^2$ two-body coupled matrix elements of this interaction attractive by 20%, the solution obtained for ^{12}C is less deformed and the $1p_{3/2}$ amplitude becomes considerably larger than the $1p_{1/2}$

amplitude thus 'effectively' increasing the spin-orbit splitting between these two levels[26]. We show the results of projection calculation for ^{12}C with Sussex and the modified Sussex interaction as described above in Fig.V(6) for the ground state band of ^{12}C. The spectrum due to the modified Sussex interaction (B) agrees well with the experimental one while the one due to unmodified Sussex interaction (A) is quite compressed. As another example, we also show the band-mixed energy spectrum (C) for ^{11}B with modified Sussex interaction by orthogonalizing three bands viz. K=1/2 oblate, K=3/2 prolate and K=3/2 oblate projected from HF intrinsic states and lying close in energy. This also agrees fairly well with the experimental spectrum. These calculations further emphasize the important role played by the spin-orbit interaction in the ^{12}C region.

V.4 Spectroscopy with band-averaged density dependent Skyrme Interaction.

We remarked in chapter II that in spite of the phenomenal success achieved with Skyrme interactions in reproducing bulk properties of nuclei, there has been very little effort in calculating spectroscopic properties such as energy spectra[27,28], transition rates etc. using such interactions. In chapter IV, we proposed a modification of Skyrme interaction in which the deformed density ρ was replaced by the band averaged scalar density ρ_0 which makes the Hamiltonian rotationally invariant and the spectros-

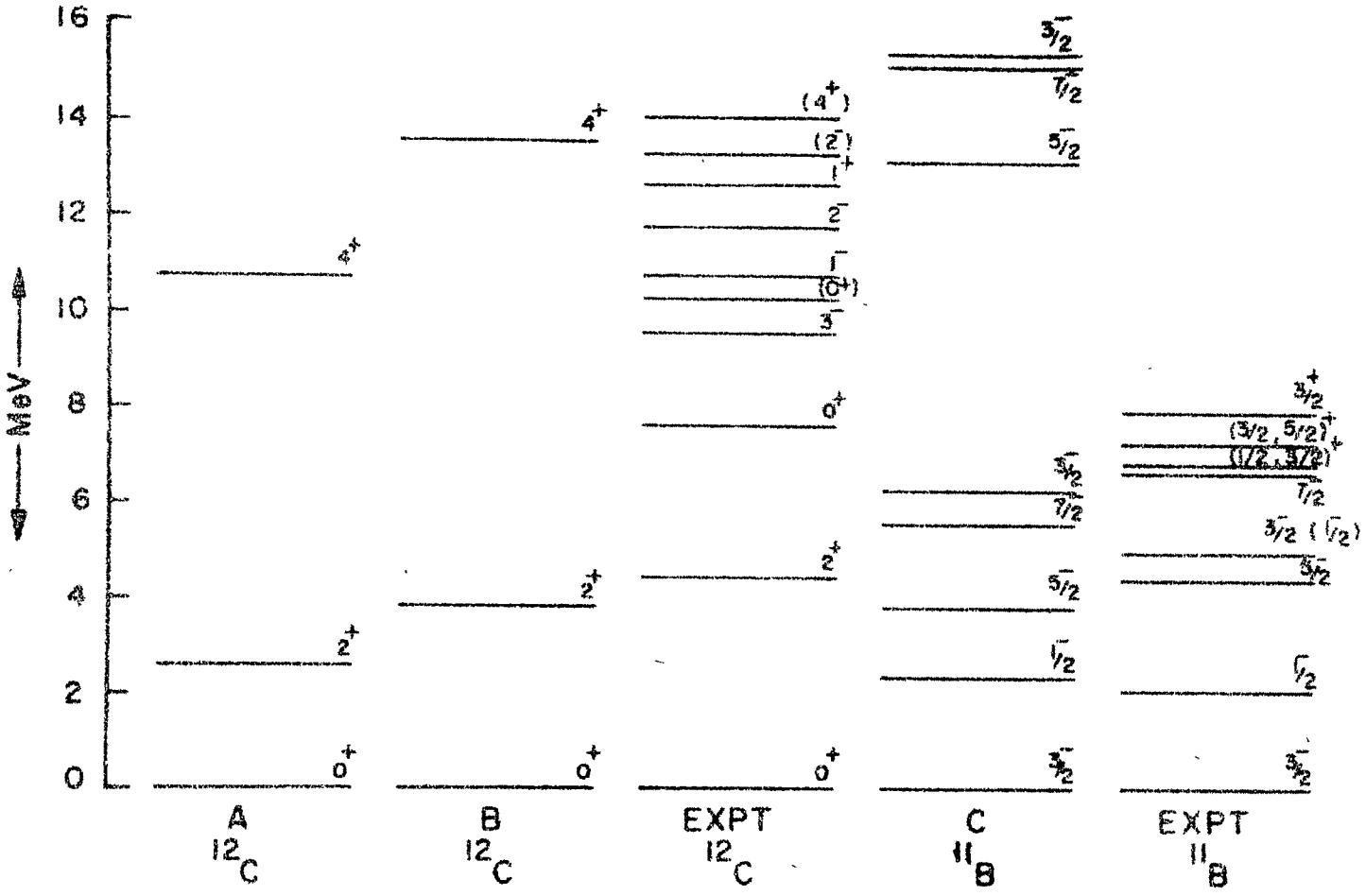

Fig.V(6): Spectra of ^{12}C and ^{11}B
(A) with unmodified Sussex interaction
(B) and (C) with modified Sussex interaction.

copic calculations are made completely feasible[29]. At the same time the agreement for the bulk properties of spherical nuclei is not disturbed. We described in chapter IV how the HF calculations for the intrinsic properties of even-even, time reversal invariant nuclei can be carried out. We reiterate that it is our aim to study the spectroscopic properties of nuclei using Skyrme interaction both density independent and density dependent in order to choose among the several variants of the Skyrme interaction.

We shall study in this section the projected ground state spectra for the nuclei ^{8}Be and ^{12}C with the interaction BASIV obtained from the HF intrinsic solutions (Tables IV.2 and IV.3) described in chapter IV. We shall deal with the nucleus ^{20}Ne separately. The projection calculations are performed with the density at which the double self-consistency between interaction matrix elements and HF wave function is achieved. We choose the variant SIV since other variants with strong density dependence pose the problem of convergence of HF solution. We remark that interactions of Skyrme-type with a strong density dependence are known to give a spherical solution[22] for ^{12}C and small alpha-clustering[30].

In Table V.2 we have given the HF intrinsic properties of ^{12}C and ^{8}Be respectively along with the energy of the 0^{+} levels in the projected spectrum for the interactions used. For the

sake of simplicity and since c.m.m. and Coulomb corrections do not affect the spectra significantly, we have not included them in our calculations[36]. It is seen that the energies in 0^+ level are several MeV lower than the HF intrinsic energies providing better agreement with experiment. In Table V.3 we give the magnetic moment and electric quadrupole moment in the state $J=2^+$ along with $B(E2, 0^+ \rightarrow 2^+)$ values for ^{12}C obtained with SV and BASIV. The agreement with available experimental data in general is quite good.

In Figs.V(7) and V(8), we show the projected ground state bands for ^{12}C and ^{8}Be with BASIV and also with SV for the sake of comparison. The 4^+ level obtained with SV for ^{12}C and ^{8}Be is calculated at a lower energy compared to the experiment. With BASIV, the 4^+ level for ^{12}C gets raised by $\sim$ 1.8 MeV and the 2^+ level is not affected thus giving excellent agreement with experiment. A similar phenomenon is seen in the case of ^{8}Be. The 4^+ level is raised as much as $\sim$ 2.5 MeV, again giving very good agreement with experiment. It is seen that 2^+ level of ^{8}Be also gets slightly lifted. BASIV thus provides a much better description than does SV.

We would like to emphasize that the introduction of scalar band averaged density dependence has made the spectroscopic calculations completely feasible removing the catastrophe caused by the three-body contact interaction as described in chapter II. We see that the introduction of density dependence dramatically raises the higher angular momentum states in both the nuclei

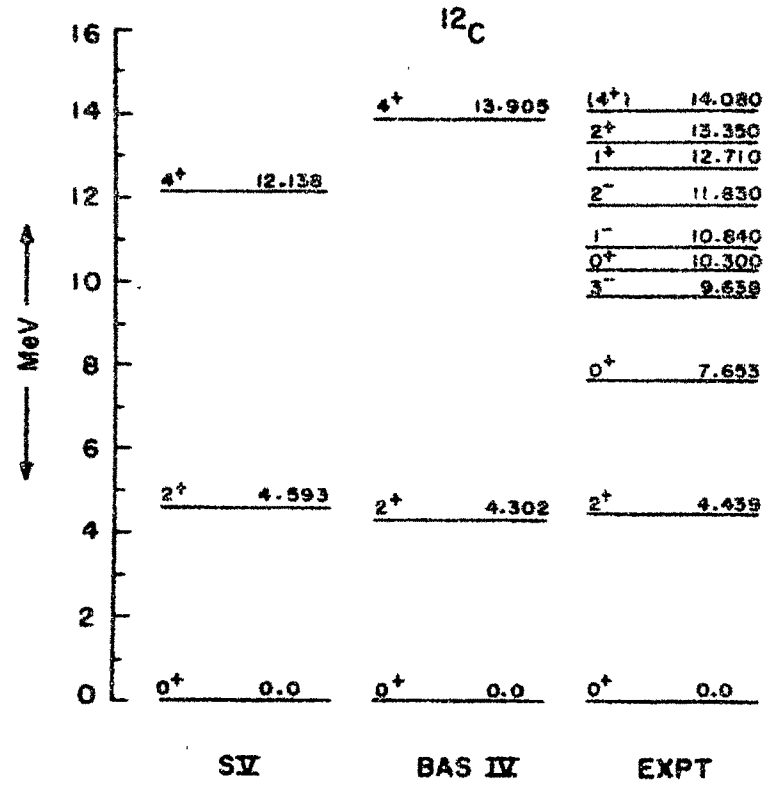

Fig.V(7): Spectra of ^{12}C with interactions SV and BASIV.

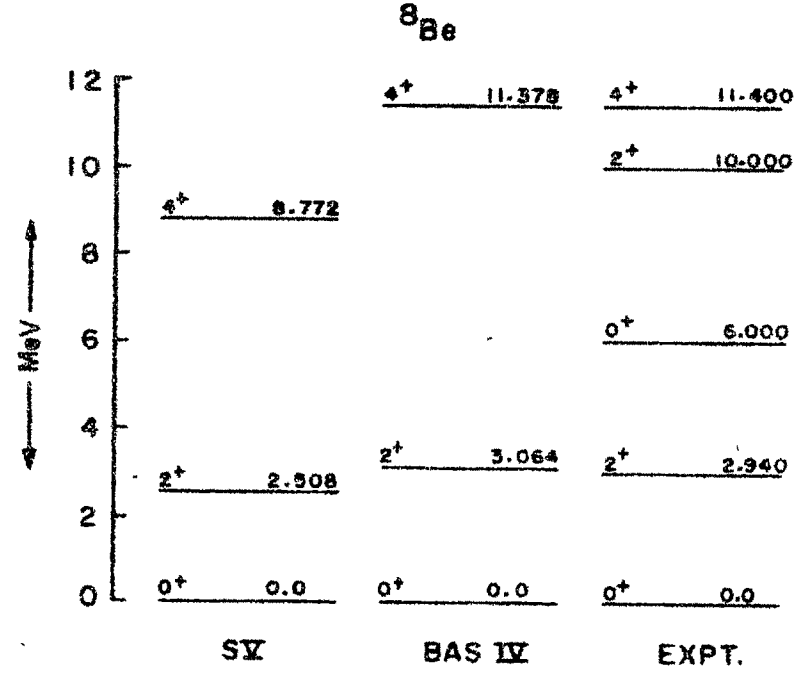

Fig.V(8): Spectra of ^{8}Be with interactions SV and BASIV.

providing excellent agreement with experiment.

V.4.1 Spectra of ^{20}Ne.

In this section we shall study the projected spectra of ^{20}Ne. Passler and Mosel[28] have performed the calculations for this nucleus in the self-consistent cranking model (CHF) using the various Skyrme variants available in the configuration space of first five major shells. It has been, however, shown[8] that CHF approximation is only a prescription to obtain the approximate behaviour of the rotational spectrum. Although the deformed density makes the Skyrme force unsuitable for rigorous spectroscopic calculations requiring good angular momentum states, Passler and Mosel use this force to calculate the rotational spectrum of ^{20}Ne. They obtain too compressed spectra with all conventional Skyrme variants. Therefore they adjust the p-state part of the interaction (the strength parameter t_2) and the s-state repulsive part (the strength parameter t_1) keeping all other parameters constant in such a way that the rotational spectrum of ^{20}Ne is obtained satisfactorily without modifying the calculated ground state energy. They obtain a reasonably good agreement for ^{20}Ne rotational spectrum with the variant SIV-d in which t_1=530 MeV fm^5 and t_2=309.3 MeV fm^5 compared to t_1=765.0 MeV fm^5 and t_2=35 MeV fm^5 in SIV with other parameters constant.

Passler and Mosel attributed the reasons for large moments of inertia and hence compressed spectra to the small p-state repulsive part (t_2) and the s-state repulsive part (t_1) of the variant SIV of the Skyrme force. They therefore increased t_2 and decreased t_1 in SIV to obtain the variant SIV-d. They obtained larger gaps with SIV-d which agrees with our results also.

We show in Table V.4 the HF intrinsic properties obtained for ^{20}Ne with SV, BASIV and BASIV-d interactions along with the energy of the 0^+ state of the ground state band. The optimized b value here is 1.9 fm which is rather large and as explained in chapter III, this is due to the severe truncational effects of the configuration space. The results of our calculations[31] for the rotational spectra of ^{20}Ne with BASIV, BASIV-d and SV are displayed in Fig.V(9) and compared with the CHF calculations of Passler and Mosel. It is seen that the variant SV gives compressed spectra in both PHF as well as CHF formalisms. It is to be noted that the interaction BASIV gives good agreement in our projected HF calculation, while CHF gives a compressed spectrum. The variant SIV-d which provides a good agreement with CHF gives a highly spread out spectrum in PHF formalism. In either case, the PHF spectrum is quite spread out compared with the CHF spectrum.

We find that BASIV provides a better description than SV for the three nuclei we have considered viz. ^{8}Be, ^{12}C and ^{20}Ne.

TABLE V.4

H.F. Results for ^{20}Ne

Interaction	E_{HF} MeV	Q_o fm^2	RMS fm	RE.EN MeV	E_{0^+} MeV
BASIV	-156.69	74.77	2.9009	-32.64	-159.77
BASIV-d	-161.1759	78.25	2.9068	-32.01	-168.75
SV	-151.52	68.17	2.8835	-	-153.51
Expt	-160.65	-	-	-	-

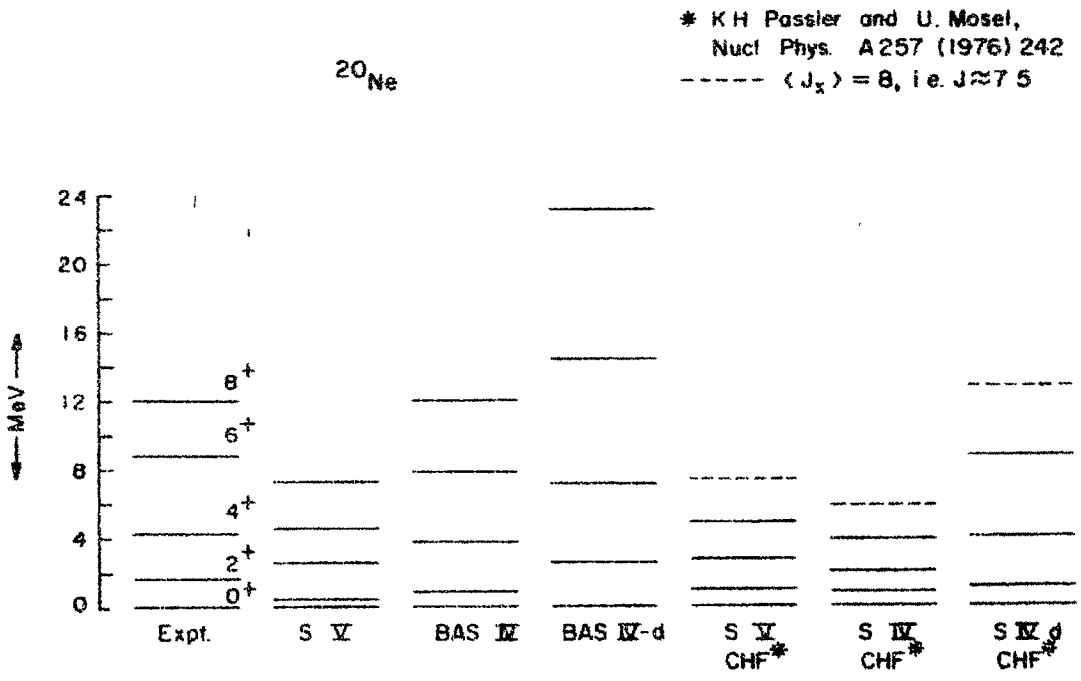

Fig.V(9): Spectra of ^{20}Ne compared with the CHF spectra

BASIV spreads out the ^{20}Ne spectrum just as in the case of ^{8}Be and ^{12}C providing good agreement with the experimental spectrum. We thus see that SIV is one Skyrme variant which provides simultaneous agreement for both bulk as well as spectroscopic properties of these nuclei. It would be quite interesting to check this point by extending these calculations to other nuclei in this region as well as heavier nuclei. This programme is being pursued.

V.5 Individual contributions of various parts of Skyrme interaction to nuclear spectra.

We saw in the preceding sections that Skyrme force provides a reasonably good agreement to the bulk properties of the even-even nuclei as well as the ground state energy spectra for ^{8}Be, ^{12}C and ^{20}Ne. In the case of ^{12}C it was shown that the two-body spin-orbit force (W) was crucial in explaining the energy spectrum. It has been shown[30] in earlier calculations that the p-state interaction term (t_2) and the three-body contact interaction term (t_3) simulating a two-body density dependent interaction affect clustering in alpha-cluster model. It is therefore quite interesting to study the individual contributions of all the terms in the Skyrme interaction to the energy spectra of nuclei. In the following we shall present the calculations for the individual contributions of various parts of Skyrme interaction to the spectra of the nuclei we have studied so far.

We shall see that most of the contribution to the energy spectra comes from the s-state atrractive (t_o) and the s-state repulsive (t_1) parts of the Skyrme interaction apart from that due to kinetic energy.

In Table V.5 we give the individual contributions of all the terms of the Skyrme interaction for the ground state K=0 bands for ^{8}Be, ^{12}C and ^{20}Ne calculated with the interaction BASIV. One can see from the table that most of the contribution to any J state comes from the s-state attractive (t_o) and s-state repulsive parts of the Skyrme interaction. The effect of other terms is quite small. The spin-orbit term (W), however, contributes significantly to the spectrum in the case of ^{12}C similar to the results obtained using the variant SV. It can be seen that the effect of the terms t_o and W is to spread out the spectrum while that of t_1, t_2 and t_3 is to compress it. The individual contribution to energy spacing of these terms is roughly proportional to their individual contributions to the binding energies. The parameters t_2 and t_3 are rather small in the variant SIV and hence such calculations with other Skyrme variants would be quite instructive to have an insight into the spectroscopic calculations with Skyrme interaction. In the present calculation, however, we see that the s-state attractive (t_o) and s-state repulsive (t_1) of the Skyrme interaction are the dominant terms which decide the overall nature of the spectrum.

TABLE V.5

Individual contribution of various parts of Skyrme interaction to the energy spectra (Interaction BASIV). All contributions in MeV.

Nucleus	J	K_E	t_0	t_1	t_2	W	t_3	Total
^{8}Be	0	111.02	-285.16	113.27	0.97	-2.55	13.28	-49.18
	2	112.33	-279.76	109.74	0.95	-2.37	13.00	-46.12
	4	116.84	-268.86	103.03	0.90	-2.05	12.32	-37.81
^{12}C	0	183.59	-470.00	176.32	4.42	-14.51	32.67	-87.50
	2	183.85	-464.30	171.96	4.27	-11.34	32.37	-83.20
	4	186.69	-450.51	162.94	4.06	-7.90	31.12	-73.60
^{20}Ne	0	313.69	-521.37	294.93	11.09	-10.13	65.71	-159.77
	2	313.85	-517.77	291.95	11.08	-9.86	65.65	-158.95
	4	314.74	-510.52	287.39	11.01	-9.31	65.34	-156.09
	6	315.96	-498.17	279.28	10.92	-8.68	64.64	-152.02
	8	317.35	-490.33	276.06	10.83	-8.39	64.04	-147.79

The effect of terms t_2 and t_3 is to change the nature such as the deformation of the intrinsic states and is indirect as far as the spectrum is concerned. However, the strength of the s-state repulsion is governed by the strength of the p-state repulsion and that of the density dependence to obtain overall agreement for the bulk properties and thus contributes in deciding the nature of the spectrum.

V.6 Summary

In this chapter, we reviewed the projection formalism and applied it to calculate the energy spectra of some light nuclei. Sussex interaction gives good agreement with experiment for the nuclei ^{8}Li, ^{8}Be and ^{8}B. The agreement obtained with the interaction SV for these nuclei may be improved by incorporating spin-orbit force properly and the density dependence. It is shown that the scalar band averaged density dependent interaction BASIV spreads out the energy spectra and provides a very good agreement with the experiment for the nuclei ^{8}Be, ^{12}C and ^{20}Ne. It was shown that the overall nature of the energy spectrum is decided by the s-state attractive and s-state repulsive parts of Skyrme interaction. The effect of the density term on the spectra is only indirect since this term and the p-state repulsive term govern the s-state repulsive term of the interaction. It was found that the two-body spin-orbit interaction is quite important in

explaining the structure of nuclei in the ^{12}C region.

In view of the above, it would be quite interesting to incorporate density dependence in spectroscopic calculations of odd and odd-odd nuclei and to extend these calculations to heavier nuclei.

REFERENCES

1. R.E. Peierls and J. Yoccoz, Proceedings of the Physical Society, 70A (1957) 381.
2. J.J. Griffin and J.A. Wheeler, Phys. Rev.108 (1957) 311.
3. D.L. Hill and J.A. Wheeler, Phys. Rev. 89 (1953) 1102.
4. Chindhu S. Warke and M.R. Gunye, Phys. Rev. 155(1967) 1084.
5. G. Ripka, Adv. Nucl. Phys. Vol.1, Plenum Press, 1968, pp.183.
6. R. Beck, H.J. Mang and P. Ring, Z.Physik, 231 (1970) 26.
7. F.M.H.Villars and N.C. Schmeing-Rogerson, Ann.of Phys. 63 (1971) 443.
8. S.K. Sharma, L. Satpathy, S.B. Khadkikar and S.C.K. Nair, Phys. Lett. 61B(1976) 122.
9. Amand Faessler, in Heavy-ion, high-spin states and Nuclear Structure, Vol.I (I.A.E.A., Vienna, 1975), pp.405.
10. D. Brink, Intern. School of Physics, "Enrico Fermi" course, Academic Press, Vol.XXXVI (1965) pp.247.
11. D. Kurath, Phys. Rev. 101 (1956) 216.
    Phys. Rev. 106 (1957) 975.
12. F.C. Barker, Nucl. Phys. 83 (1966) 418.
13. D. Amit and A. Katz, Nucl. Phys. 58 (1964) 388.
    Nucl. Phys. 71 (1965) 696.
14. S. Cohen and D. Kurath, Nucl. Phys. 73 (1965) 1
    89(1966) 707
    A101(1967) 1
    A141(1970) 145.

15. N. Kumar, Nucl. Phys.A225 (1974) 221.

16. H. Dirim, J.P. Elliott and J.A. Evans, Nucl. Phys. A244 (1975) 301.

17. E.A. Sanderson, J.P. Elliott, H.A. Mavrometis and B. Singh Nucl. Phys. A219 (1974) 190.

18. M.R. Gunye, J. Law and R.K. Bhaduri, Nucl. Phys. A132 (1969) 225.

19. V.B. Kamble and S.B. Khadkikar, Proceedings of Nuclear Physics and Solid State Physics Symposium, Calcutta,India, Dec.22-26, 1975, pp.213, Vol.18B.

20. S.B. Khadkikar, V.B. Kamble and D.R. Kulkarni, Proceedings of the International Conference on Nuclear Self-consistent Fields, I.C.T.P., Trieste, Italy, Feb.24-28, 1975, edited by G. Ripka and M. Porneuf, North Holland Publishing Company, pp.85.

21. D. Vautherin, Phys. Rev. C7 (1973) 296.

22. J.L. Friar and J.W. Negele, Nucl. Phys. A240 (1975) 301.

23. R. Behrman, S. Das Gupta and N.De Takacsy, in Proc. Intern. Conf.on Nuclear Physics, Munich, 1973, pp.114.

24. H. Friedrich and A. Weigury, Phys. Lett. 35B (1971) 105.

25. V.B. Kamble and S.B. Khadkikar, Phys. Lett. 59B(1975) 19.

26. V.B. Kamble, S.B. Khadkikar and D.R. Kulkarni, Nuclear Physics and Solid State Physics Symposium, Calcutta,India, Dec.22-26, 1975, pp.216, Vol.18B.

27. G.F. Bertsch and S.F. Tsai, Phys. Rep. 18, No.2, 125 (1975).

28. K.H. Passler and U. Mosel, Nucl. Phys. A257 (1976) 242.

29. S.B. Khadkikar and V.B. Kamble, Phys. Lett. 64B(1976) 131.

30. S.B. Khadkikar, Phys. Lett. 36B (1971) 451.

31. V.B. Kamble and S.B. Khadkikar, Nuclear Physics and Solid State Physics Symposium, Ahmedabad, India, Dec.27-31, 1976, to be published.

32. V.B. Kamble and S.B. Khadkikar, ibid.

33. H. Trivedi, Private communication.

34. H.A. Bentz, Z. Naturf. 24a (1969) 858.

35. S.J. Skorka, J. Hertel and J.W. Retz-Schmidt, Nucl. Data 2 (1967) 342.

36. V.B. Kamble, S.B. Khadkikar and D.R. Kulkarni, Nuclear Physics and Solid State Physics Symposium, B.A.R.C., Bombay, India, Dec. 27-31, 1974, pp.204, Vol.17B.

37. R.C. Haskell and L. Madansky, Phys. Rev. C7(1973) 1277.

38. T. Minamisono, Y. Nojiri, A. Mizobuchi and K.Sugimoto, J. Phys. Soc. Japan 34, Suppl. (1973) 156, 324.

39. H. Ackermann, D. Dubbers, M. Grupp, P. Heitjans and H.J. Stockmann, Phys. Lett. 52B (1974) 54.